particles

IMPACT FACTOR 1.7

CITESCORE 3.2

Article

# Magic Number $N = 350$ Predicted by the Deformed Relativistic Hartree-Bogoliubov Theory in Continuum: $Z = 136$ Isotopes as an Example

Wei-Jian Liu, Chen-Jun Lv, Peng Guo, Cong Pan, Sibo Wang and Xin-Hui Wu

Special Issue

Selected Papers from the "7th Workshop on the Nuclear Mass Table with DRHBc Theory"

Edited by

Dr. Shuangquan Zhang and Dr. Youngman Kim

MDPI

https://doi.org/10.3390/particles7040065

*particles*

MDPI

*Article*

# Magic Number $N = 350$ Predicted by the Deformed Relativistic Hartree-Bogoliubov Theory in Continuum: $Z = 136$ Isotopes as an Example

**Wei-Jian Liu [1], Chen-Jun Lv [1], Peng Guo [2], Cong Pan [3,4], Sibo Wang [5,6] and Xin-Hui Wu [1,2,*]**

[1] Department of Physics, Fuzhou University, Fuzhou 350108, China; 052203115@fzu.edu.cn (W.-J.L.)
[2] State Key Laboratory of Nuclear Physics and Technology, School of Physics, Peking University, Beijing 100871, China; 2301110125@pku.edu.cn
[3] Department of Physics, Anhui Normal University, Wuhu 241000, China; cpan@ahnu.edu.cn
[4] Center for Exotic Nuclear Studies, Institute for Basic Science, Daejeon 34126, Republic of Korea
[5] Department of Physics, Chongqing University, Chongqing 401331, China
[6] Chongqing Key Laboratory for Strongly Coupled Physics, Chongqing 401331, China
* Correspondence: wuxinhui@fzu.edu.cn

**Abstract:** The investigation of magic numbers for nuclei in the hyperheavy region ($Z > 120$) is an interesting topic. The neutron magic number $N = 350$ is carefully validated by the deformed relativistic Hartree-Bogoliubov theory in continuum (DRHBc), via analysing even-even nuclei around $N = 350$ of the $Z = 136$ isotopes in detail. Nuclei with $Z = 136$ and $340 \leq N \leq 360$ are all found to be spherical in their ground states. A big drop of the two-neutron separation energy $S_{2n}$ is observed from $N = 350$ to $N = 352$ in the isotopic chain of $Z = 136$, and a peak of the two-neutron gap $\delta_{2n}$ appears at $N = 350$. There exists a big shell gap above $N = 350$ around the spherical regions of single-neutron levels for nucleus with $(Z = 136, N = 350)$. These evidences from the DRHBc theory support $N = 350$ to be a neutron magic number in the hyperheavy region.

**Keywords:** relativistic density functional theory; deformed relativistic Hartree-Bogoliubov theory in continuum; magic number; hyperheavy nuclei

check for updates

**Citation:** Liu, W.-J.; Lv, C.-J.; Guo, P.; Pan, C.; Wang, S.; Wu, X.-H. Magic Number $N = 350$ Predicted by the Deformed Relativistic Hartree-Bogoliubov Theory in Continuum: $Z = 136$ Isotopes as an Example. *Particles* **2024**, *7*, 1078–1085. https://doi.org/10.3390/particles7040065

Academic Editors: Shuangquan Zhang, Youngman Kim and Armen Sedrakian

Received: 29 September 2024
Revised: 20 November 2024
Accepted: 21 November 2024
Published: 26 November 2024

**Copyright:** © 2024 by the authors. Licensee MDPI, Basel, Switzerland. This article is an open access article distributed under the terms and conditions of the Creative Commons Attribution (CC BY) license (https://creativecommons.org/licenses/by/4.0/).

## 1. Introduction

The investigation of superheavy elements remains one of the most important topics of nuclear physics and chemistry. The element with the largest proton number $Z$ observed so far is Og with $Z = 118$ [1]. The limit of the existence of atomic nuclei is a longstanding issue for both experimental and theoretical nuclear physicists, and has important impacts on physics and chemistry. The nuclei with $Z > 120$ are usually called hyperheavy nuclei [2]. The studies of hyperheavy nuclei can enhance our understanding of exotic nuclear structures and enable the delving into the limits of charge and mass of atomic nuclei.

Nuclear liquid drop model (LDM) [3] can help us obtain a quick understanding of the hyperheavy nuclei, which suggests the importance of the competition between Coulomb energies and surface effects in the hyperheavy region. However, due to the lack of quantum shell effect, the predictions given by the LDM are pretty rough. Quantum shell effect, which corresponds to a non-uniformity distribution of the individual single-particle energies, is very important for finite nuclear systems. It can produce a significant energy gap in the single-particle energy spectrum near the Fermi level for some nuclei. Such gaps would provide additional binding energies and enhance nuclear stability. These nuclei with additional stability are the so-called "magic nuclei", and the corresponding proton or neutron numbers are called "magic numbers". Experimentally, the confirmed neutron magic numbers are 8, 20, 28, 50, 82, 126, and the confirmed proton magic numbers are 8, 20, 28, 50, 82.

Due to the additional stability, magic nuclei have drawn a lot of attention [4,5]. Naïvely, if one assumes the potential for nucleons within an atomic nucleus is a harmonic oscillator potential, the obtained magic numbers will be 2, 8, 20, 40, 70, 112, 168, 240, ..., which disagree with experiments. If one further takes into account the spin-orbital coupling, the predicted magic numbers are 2, 8, 20, 28, 50, 82, 126, 184, 258, 350, ..., which correctly reproduce the experimental magic numbers for $N \leq 126$ and $Z \leq 82$. However, due to the limit of experimental information, the large predicted magic numbers, such as 258 and 350, are difficult to be validated in the foreseeable future. For hyperheavy nuclei with $Z > 120$, the neutron numbers of which can reach to $N \approx 350$, and it will be interesting to use a microscopic and self-consistent model to theoretically justify the predicted neutron magic number 350.

Nuclear stability is usually described by the binding energy or equivalently nuclear mass. Nuclear mass is important for both nuclear physics [6,7] and astrophysics [8–11]. Experimentally, the masses of about 2500 nuclear masses have been measured to date [12]. Theoretically, many nuclear models [13–24] and machine-learning approaches [25–36] are developed to predict nuclear masses. Among these models, the deformed relativistic Hartree-Bogoliubov theory in continuum (DRHBc) [37,38] simultaneously treats the deformation degrees of freedom, pairing correlations, and continuum effects properly, which are important for the descriptions of weakly bound exotic nuclei. The DRHBc theory has been successfully applied in studying many nuclear phenomena [39–56]. In order to provide a unified and microscopic description for the whole nuclear landscape, the DRHBc Mass Table Collaboration [57] was established, aiming at establishing a nuclear mass table based on the DRHBc theory with the density functional PC-PK1 [58]. The even-even [22] and even-odd [24] parts of the DRHBc mass table have been established recently. The Collaboration is now working on odd-$Z$ nuclei and hyperheavy nuclei with $120 < Z \leq 136$. Taking this opportunity, one can validate the neutron magic number $N = 350$ with the DRHBc theory. In this work, the DRHBc theory is employed to study the even nuclei of $Z = 136$ isotopes around $N = 350$ to validate the possible neutron magic number $N = 350$. To our knowledge, there is currently no literature that employs modern nuclear model to study the neutron magic number $N = 350$. In Section 2, the theoretical framework is introduced. The numerical details are introduced in Section 3. The Results and discussions are presented in Section 4. Finally, a summary is given in Section 5.

## 2. Theoretical Framework

The details of the DRHBc theory with meson-exchange and point-coupling density functionals can be found in Refs. [38,59], respectively. In the following we briefly present its formalism.

Treating self-consistently the mean fields and pairing correlations, the relativistic Hartree Bogoliubov (RHB) equations for the nucleons read [60]

$$\begin{pmatrix} h_D - \lambda_\tau & \Delta \\ -\Delta^* & -h_D^* + \lambda_\tau \end{pmatrix} \begin{pmatrix} U_k \\ V_k \end{pmatrix} = E_k \begin{pmatrix} U_k \\ V_k \end{pmatrix}. \tag{1}$$

To describe properly the possible large spatial extension of exotic nuclei, the RHB equations are solved in a Dirac Woods-Saxon basis, in which the radial wave functions have a proper asymptotic behavior for large $r$ [61]. In Equation (1), $\lambda_\tau$ is the Fermi energy ($\tau = n/p$ for neutrons or protons), $E_k$ and $(U_k, V_k)^{\mathrm{T}}$ the quasiparticle energy and wave function, and $h_D$ the Dirac Hamiltonian,

$$h_D(\boldsymbol{r}) = \boldsymbol{\alpha} \cdot \boldsymbol{p} + V(\boldsymbol{r}) + \beta[M + S(\boldsymbol{r})], \tag{2}$$

with the scalar $S(\boldsymbol{r})$ and vector $V(\boldsymbol{r})$ potentials. The pairing potential $\Delta$ reads

$$\Delta(\boldsymbol{r}_1, \boldsymbol{r}_2) = V^{\mathrm{pp}}(\boldsymbol{r}_1, \boldsymbol{r}_2)\kappa(\boldsymbol{r}_1, \boldsymbol{r}_2), \tag{3}$$

with a density-dependent force of zero range,

$$V^{\mathrm{pp}}(\boldsymbol{r}_1,\boldsymbol{r}_2) = V_0\frac{1}{2}(1-P^{\sigma})\delta(\boldsymbol{r}_1-\boldsymbol{r}_2)\left(1-\frac{\rho(\boldsymbol{r}_1)}{\rho_{\mathrm{sat}}}\right), \tag{4}$$

and the pairing tensor $\kappa$ [62]. For axially deformed nuclei, the potentials and densities are expanded in terms of the Legendre polynomials,

$$f(\boldsymbol{r}) = \sum_{\lambda} f_{\lambda}(r)P_{\lambda}(\cos\theta), \quad \lambda = 0,2,4,\cdots, \tag{5}$$

where $\lambda$ is restricted to be even numbers due to spatial reflection symmetry.

## 3. Numerical Details

In Equation (4), the pairing strength $V_0 = -325$ MeV fm$^3$, the saturation density $\rho_{\mathrm{sat}} = 0.152$ fm$^{-3}$, and a pairing window of 100 MeV are adopted. The energy cutoff $E^{+}_{\mathrm{cut}}$ = 300 MeV and the angular momentum cutoff $J_{\mathrm{max}}$ = 23/2 $\hbar$ are adopted for the Dirac Woods-Saxon basis. In Equation (5), the Legendre expansion is truncated at $\lambda_{\mathrm{max}} = 10$ [63]. The calculations are carried out with the relativistic density functional PC-PK1 [58]. These numerical details are the same as the calculations of nuclei with $100 \leq Z \leq 120$ in the global DRHBc mass table calculations over the nuclear chart [22,24,59], and have also been examined to be proper for the studies in this work.

## 4. Results and Discussions

Evolution of the potential energy curves (PECs) of $Z = 136$ isotopes with $340 \leq N \leq 360$ is presented in Figure 1. Note that the $Z = 136$ element has temporary systematic IUPAC name and symbol as Untrihexium and Uth respectively [64]. One can see the similar behaviours of these PECs, where the total energy increases monotonously with the increasing absolute value of $\beta_2$ in the range that $|\beta_2| < 0.3$, indicating that these nuclei are spherical in their ground states. Note that the cutoff of angular momentum has been examined in Ref. [65], which suggests $J_{max} = 31/2\,\hbar$ in the calculation of the hyperheavy nuclei ($121 \leq Z \leq 136$) with quadruple deformation $|\beta_2| > 0.3$. The spherical ground states of these nuclei can be interpreted as a clue that $N = 350$ (or other adjacent neutron numbers) is a neutron magic number, since atomic nuclei prefer to be spherical around the magic ones. Note that the nuclei that are analyzed in the present work all have spherical ground states, which might lead one to consider $Z = 136$ as a potential magic number. However, we have checked the nuclei that are not close to $N = 350$ in $Z = 136$ isotopic chain, most of which are not spherical ones. We have also checked the single-proton levels around the Fermi level of $^{486}$Uth , and there is not a significant gap above $Z = 136$. Instead, there is a significant gap above $Z = 138$, which may suggest 138 to be a proton magic number. However, this is out of the scope of the present paper, which could be an interesting topic for the future work.

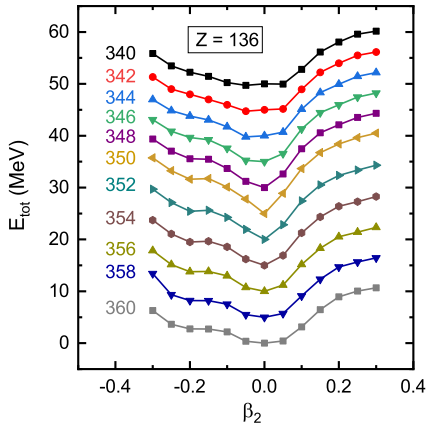


**Figure 1.** Evolution of the potential energy curves (PECs) of Uth ($Z = 136$) isotopes with $340 \leq N \leq 360$. For clarity reasons, the curves have been scaled to the energy of $\beta_2 = 0$ and have been shifted upward by 5 MeV per decreasing two neutrons.

In order to pin down which neutron number is the magic one, the two-neutron separation energies $S_{2n}$ and Fermi energies $\lambda_n$ for these Uth isotopes are presented in Figure 2. One can see that the two-neutron separation energies $S_{2n}$ evolve slowly with the increasing of neutron number from $N = 340$ to $N = 350$ and from $N = 352$ to $N = 360$. However, there is a big drop in the $S_{2n}$ from $N = 350$ to $N = 352$. This indicates that there is a big shell gap at $N = 350$, which is a strong evidence for a magic number. There is also a big jump in the Fermi energies $\lambda_n$ from $N = 350$ to $N = 352$, which leads to the same conclusion. Two-neutron gap $\delta_{2n} = S_{2n}(N, Z) - S_{2n}(N + 2, Z)$ is also a very good signature of magic numbers. As can be clearly seen in Figure 2, a peak of $\delta_{2n}$ appears at $N = 350$.

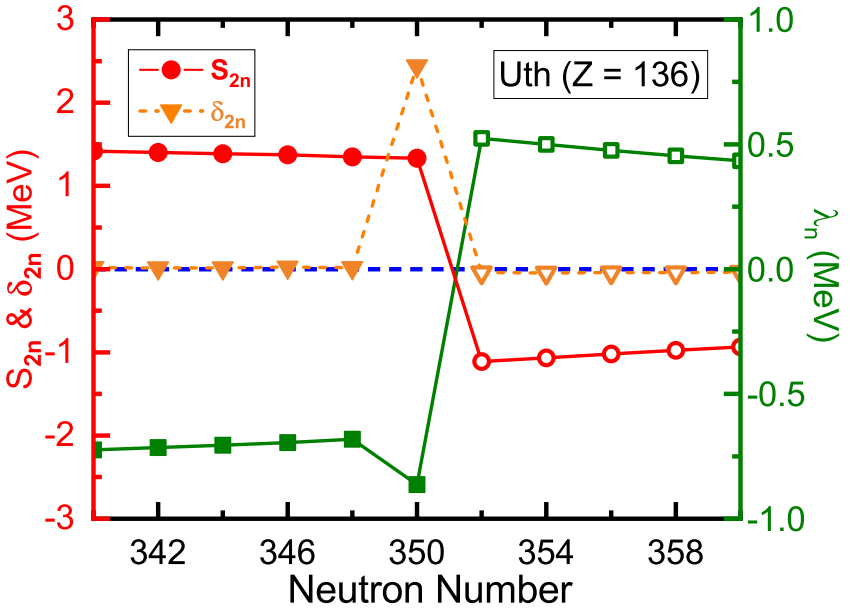


**Figure 2.** Two-neutron separation energies $S_{2n}$, two-neutron gaps $\delta_{2n}$, and Fermi energies $\lambda_n$ for the Uth $(Z = 136)$ isotopes with $340 \leq N \leq 360$. The bound nuclei predicted by the DRHBc theory are denoted by filled circles, while the unbound nuclei are denoted by empty circles. The blue dashed line displays $S_{2n} = 0$, $\delta_{2n} = 0$, and $\lambda_n = 0$.

Neutron magic nuclei are typically more stable than their next neutron-rich neighbors, while the neutron-richer nuclei next to the magic nuclei are much more likely to emit extra neutrons outside the shells. One can also see in Figure 2 that the $S_{2n}$ of nuclei $N \geq 352$ are smaller than zero, which means that these nuclei are unstable against neutron emission. The corresponding Fermi energies for these nuclei are larger than 0, which also refers to the unstable characters. Therefore, the neutron drip-line nucleus of Uth isotopic chain locates at $N = 350$. Note that the Coulomb repulsion will be very large in superheavy and hyperheavy nuclei, and tends to prevent the nuclear binding. The reason why such a hyperheavy nucleus $^{486}$Uth still can be bound is due to strong shell effect. The shell effect is a hallmark characteristic in the atomic nucleus as a quantum system, providing extra binding that can overcome Coulomb repulsion and makes the nucleus bound.

In order to confirm the neutron magic number, the single-neutron levels around the Fermi level should be carefully checked. Figure 3 shows the single-neutron levels around the Fermi level of $^{486}$Uth in the canonical basis obtained from constraint calculations. One can find a big gap above $N = 350$ around the spherical regions, i.e., $-0.05 < \beta_2 < 0.05$. This strongly supports $N = 350$ as a neutron magic number.

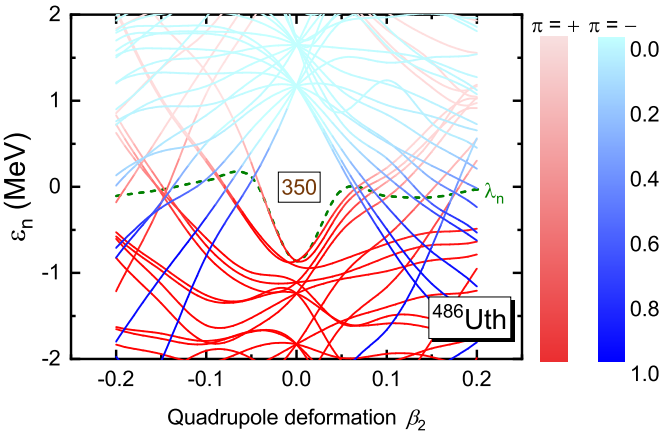


**Figure 3.** Single-neutron levels around the Fermi level of $^{486}$Uth in the canonical basis obtained from constraint calculations with the DRHBc theory. The occupation probability of each orbital is represented with different colors. The Fermi level $\lambda_n$ is displayed by the green dashed line.

Figure 4 provides single-neutron and single-proton levels around the Fermi levels for the spherical ground state of $^{486}$Uth, and the corresponding spherical quantum numbers are labeled. As can be seen, the big gap of $N = 350$ appears between the level $4d_{3/2}$ and $1I_{17/2}$. In the future works, it would be interesting to check the model dependence of neutron magic number $N = 350$, as well as the related levels, among different methods and different functionals employed.

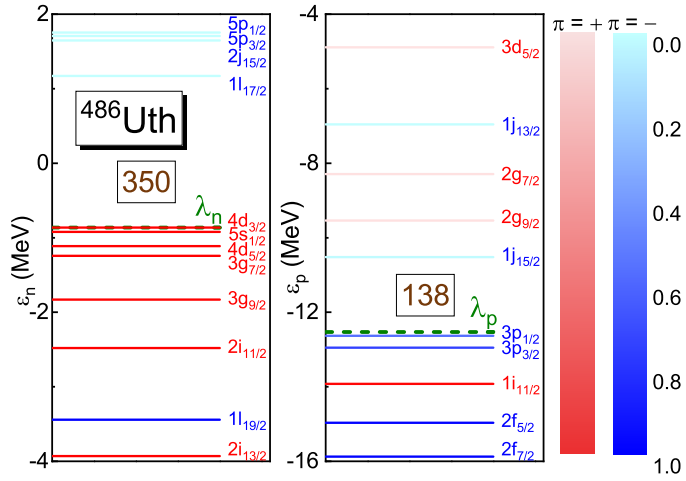


**Figure 4.** Single-neutron and single-proton levels around the Fermi levels for the spherical ground state of $^{486}$Uth in the canonical basis obtained with the DRHBc theory. The occupation probability of each orbital is represented with different colors. The Fermi levels $\lambda_n, \lambda_p$ are displayed by the green dashed lines. The spherical quantum numbers are given for corresponding levels.

## 5. Summary

The investigation of magic numbers of hyperheavy nuclei is an interesting topic. The neutron number $N = 350$ is predicted to be a magic number by the naïve analysis based on harmonic oscillator potential with spin-orbital coupling. In this work, the predicted neutron magic number $N = 350$ is validated with the DRHBc theory by studying the Uth ($Z = 136$) isotopes around $N = 350$. It is found that the Uth isotopes with $340 \leq N \leq 360$ are all spherical in their ground states. A big drop of the $S_{2n}$ appears from $N = 350$ to $N = 352$, and a peak of $\delta_{2n}$ is observed at $N = 350$. By taking $^{486}$Uth as an example, in the single-neutron levels, there exists a big shell gap above $N = 350$ around the spherical regions, i.e., $-0.05 < \beta_2 < 0.05$. These evidences from DRHBc theory all support $N = 350$ to be a neutron magic number in the hyperheavy region.

Note that we presently focus on $Z = 136$ isotopic chain as an example, and a more rigorous validation of neutron magic number should be examined also for other isotopic chains. The preliminary results of other isotopic chains in the hyperheavy region from the DRHBc theory also support $N = 350$ to be a neutron magic number. A more comprehensive investigation could be carried out in the future to analyze all the results of hyperheavy nuclei. In that case, one could have a more rigorous validation of neutron magic number $N = 350$ and also other possible neutron and proton magic numbers in the hyperheavy region. Considering that the present calculations with the DRHBc theory assume nuclei to be axial symmetry and base on the PC-PK1 functional, it would be interesting to investigate the evolution of shell gaps with triaxial deformation or with octupole deformation, to validate whether the triaxial or octupole deformations can challenge the spherical minima of these nuclei. It would also be interesting to check the functional dependence of neutron magic number $N = 350$.

**Author Contributions:** Conceptualization, X.-H.W.; methodology, C.P. and P.G.; formal analysis, C.P., P.G. and S.W.; investigation, W.-J.L. and C.-J.L.; writing—original draft preparation, X.-H.W.; writing—review and editing, All authors; visualization, W.-J.L., C.-J.L. and X.-H.W.; supervision, X.-H.W.; project administration, X.-H.W.; funding acquisition, S.W. and X.-H.W. All authors have read and agreed to the published version of the manuscript.

**Funding:** This work was partly supported by the National Natural Science Foundation of China under Grant No. 12405134 and No. 12205030, the State Key Laboratory of Nuclear Physics and Technology, Peking University under Grant No. NPT2023KFY02, the China Postdoctoral Science Foundation under Grant No. 2021M700256, and the start-up grant XRC-23103 of Fuzhou University.

**Data Availability Statement:** The dataset can be accessed upon request to the corresponding author.

**Acknowledgments:** Helpful discussions with members of the DRHBc Mass Table Collaboration are highly appreciated.

**Conflicts of Interest:** The authors declare no conflicts of interest.

## References

1. Oganessian, Y.T.; Abdullin, F.S.; Alexander, C.; Binder, J.; Boll, R.A.; Dmitriev, S.N.; Ezold, J.; Felker, K.; Gostic, J.M.; Grzywacz, R.K.; et al. Production and Decay of the Heaviest Nuclei $^{293,294}117$ and $^{294}118$. *Phys. Rev. Lett.* **2012**, *109*, 162501. [CrossRef] [PubMed]
2. Dechargé, J.; Berger, J.F.; Dietrich, K.; Weiss, M. Superheavy and hyperheavy nuclei in the form of bubbles or semi-bubbles. *Phys. Lett. B* **1999**, *451*, 275–282. [CrossRef]
3. Weizsäcker, C.F.V. Zur Theorie der Kernmassen. *Z. Phys.* **1935**, *96*, 431–458. [CrossRef]
4. Sorlin, O.; Porquet, M.G. Nuclear magic numbers: New features far from stability. *Prog. Part. Nucl. Phys.* **2008**, *61*, 602–673. [CrossRef]
5. Otsuka, T.; Gade, A.; Sorlin, O.; Suzuki, T.; Utsuno, Y. Evolution of shell structure in exotic nuclei. *Rev. Mod. Phys.* **2020**, *92*, 015002. [CrossRef]
6. Lunney, D.; Pearson, J.M.; Thibault, C. Recent trends in the determination of nuclear masses. *Rev. Mod. Phys.* **2003**, *75*, 1021–1082. [CrossRef]
7. Yamaguchi, T.; Koura, H.; Litvinov, Y.; Wang, M. Masses of exotic nuclei. *Prog. Part. Nucl. Phys.* **2021**, *120*, 103882. [CrossRef]
8. Mumpower, M.; Surman, R.; McLaughlin, G.; Aprahamian, A. The impact of individual nuclear properties on r-process nucleosynthesis. *Prog. Part. Nucl. Phys.* **2016**, *86*, 86–126. [CrossRef]
9. Jiang, X.F.; Wu, X.H.; Zhao, P.W. Sensitivity Study of r-process Abundances to Nuclear Masses. *Astrophys. J.* **2021**, *915*, 29. [CrossRef]
10. Wu, X.H.; Zhao, P.W.; Zhang, S.Q.; Meng, J. High-precision Nuclear Chronometer for the Cosmos. *Astrophys. J.* **2022**, *941*, 152. [CrossRef]
11. Wu, X.H.; Meng, J. Supporting the CMB cosmic age from nuclear physics. *Sci. Bull.* **2023**, *68*, 539–541. [CrossRef] [PubMed]
12. Wang, M.; Huang, W.; Kondev, F.; Audi, G.; Naimi, S. The AME 2020 atomic mass evaluation (II). Tables, graphs and references. *Chin. Phys. C* **2021**, *45*, 030003. [CrossRef]
13. Pearson, J.; Nayak, R.; Goriely, S. Nuclear mass formula with Bogolyubov-enhanced shell-quenching: Application to r-process. *Phys. Lett. B* **1996**, *387*, 455–459. [CrossRef]
14. Wang, N.; Liu, M.; Wu, X.; Meng, J. Surface diffuseness correction in global mass formula. *Phys. Lett. B* **2014**, *734*, 215–219. [CrossRef]

15. Möller, P.; Sierk, A.; Ichikawa, T.; Sagawa, H. Nuclear ground-state masses and deformations: FRDM(2012). *At. Data Nucl. Data Tables* **2016**, *109–110*, 1–204. [CrossRef]
16. Koura, H.; Tachibana, T.; Uno, M.; Yamada, M. Nuclidic Mass Formula on a Spherical Basis with an Improved Even-Odd Term. *Prog. Theor. Phys.* **2005**, *113*, 305–325. [CrossRef]
17. Goriely, S.; Chamel, N.; Pearson, J.M. Skyrme-Hartree-Fock-Bogoliubov Nuclear Mass Formulas: Crossing the 0.6 MeV Accuracy Threshold with Microscopically Deduced Pairing. *Phys. Rev. Lett.* **2009**, *102*, 152503. [CrossRef]
18. Goriely, S.; Hilaire, S.; Girod, M.; Péru, S. First Gogny-Hartree-Fock-Bogoliubov Nuclear Mass Model. *Phys. Rev. Lett.* **2009**, *102*, 242501. [CrossRef]
19. Peña-Arteaga, D.; Goriely, S.; Chamel, N. Relativistic mean-field mass models. *Eur. Phys. J.* **2016**, *52*, 320. [CrossRef]
20. Xia, X.; Lim, Y.; Zhao, P.; Liang, H.; Qu, X.; Chen, Y.; Liu, H.; Zhang, L.; Zhang, S.; Kim, Y.; et al. The limits of the nuclear landscape explored by the relativistic continuum Hartree–Bogoliubov theory. *At. Data Nucl. Data Tables* **2018**, *121–122*, 1–215. [CrossRef]
21. Yang, Y.L.; Wang, Y.K.; Zhao, P.W.; Li, Z.P. Nuclear landscape in a mapped collective Hamiltonian from covariant density functional theory. *Phys. Rev. C* **2021**, *104*, 054312. [CrossRef]
22. Zhang, K.; Cheoun, M.K.; Choi, Y.B.; Chong, P.S.; Dong, J.; Dong, Z.; Du, X.; Geng, L.; Ha, E.; He, X.T.; et al. Nuclear mass table in deformed relativistic Hartree–Bogoliubov theory in continuum, I: Even–even nuclei. *At. Data Nucl. Data Tables* **2022**, *144*, 101488. [CrossRef]
23. Pan, C.; Cheoun, M.K.; Choi, Y.B.; Dong, J.; Du, X.; Fan, X.H.; Gao, W.; Geng, L.; Ha, E.; He, X.T.; et al. Deformed relativistic Hartree-Bogoliubov theory in continuum with a point-coupling functional. II. Examples of odd Nd isotopes. *Phys. Rev. C* **2022**, *106*, 014316. [CrossRef]
24. Guo, P.; Cao, X.; Chen, K.; Chen, Z.; Cheoun, M.K.; Choi, Y.B.; Lam, P.C.; Deng, W.; Dong, J.; Du, P.; et al. Nuclear mass table in deformed relativistic Hartree–Bogoliubov theory in continuum, II: Even-Z nuclei. *At. Data Nucl. Data Tables* **2024**, *158*, 101661. [CrossRef]
25. Utama, R.; Piekarewicz, J.; Prosper, H.B. Nuclear mass predictions for the crustal composition of neutron stars: A Bayesian neural network approach. *Phys. Rev. C* **2016**, *93*, 014311. [CrossRef]
26. Neufcourt, L.; Cao, Y.; Nazarewicz, W.; Olsen, E.; Viens, F. Neutron Drip Line in the Ca Region from Bayesian Model Averaging. *Phys. Rev. Lett.* **2019**, *122*, 062502. [CrossRef]
27. Wu, X.H.; Zhao, P.W. Predicting nuclear masses with the kernel ridge regression. *Phys. Rev. C* **2020**, *101*, 051301. [CrossRef]
28. Wu, X.H.; Guo, L.H.; Zhao, P.W. Nuclear masses in extended kernel ridge regression with odd-even effects. *Phys. Lett. B* **2021**, *819*, 136387. [CrossRef]
29. Guo, L.H.; Wu, X.H.; Zhao, P.W. Nuclear Mass Predictions of the Relativistic Density Functional Theory with the Kernel Ridge Regression and the Application to r-Process Simulations. *Symmetry* **2022**, *14*, 1078. [CrossRef]
30. Wu, X.H.; Lu, Y.Y.; Zhao, P.W. Multi-task learning on nuclear masses and separation energies with the kernel ridge regression. *Phys. Lett. B* **2022**, *834*, 137394. [CrossRef]
31. Du, X.K.; Guo, P.; Wu, X.H.; Zhang, S.Q. Examination of machine learning for assessing physical effects: Learning the relativistic continuum mass table with kernel ridge regression*. *Chin. Phys. C* **2023**, *47*, 074108. [CrossRef]
32. Wu, X.H.; Pan, C.; Zhang, K.Y.; Hu, J. Nuclear mass predictions of the relativistic continuum Hartree-Bogoliubov theory with the kernel ridge regression. *Phys. Rev. C* **2024**, *109*, 024310. [CrossRef]
33. Niu, Z.M.; Liang, H.Z. Nuclear mass predictions with machine learning reaching the accuracy required by *r*-process studies. *Phys. Rev. C* **2022**, *106*, L021303. [CrossRef]
34. Li, M.; Sprouse, T.M.; Meyer, B.S.; Mumpower, M.R. Atomic masses with machine learning for the astrophysical r process. *Phys. Lett. B* **2024**, *848*, 138385. [CrossRef]
35. Wu, X.H.; Zhao, P.W. Principal components of nuclear mass models. *Sci. China-Phys. Mech. Astron.* **2024**, *67*, 272011. [CrossRef]
36. Wu, X.H.; Pan, C. Nuclear mass predictions with anisotropic kernel ridge regression. *Phys. Rev. C* **2024**, *110*, 034322. [CrossRef]
37. Zhou, S.G.; Meng, J.; Ring, P.; Zhao, E.G. Neutron halo in deformed nuclei. *Phys. Rev. C* **2010**, *82*, 011301. [CrossRef]
38. Li, L.; Meng, J.; Ring, P.; Zhao, E.G.; Zhou, S.G. Deformed relativistic Hartree-Bogoliubov theory in continuum. *Phys. Rev. C* **2012**, *85*, 024312. [CrossRef]
39. Sun, X.X. Deformed two-neutron halo in $^{19}$B. *Phys. Rev. C* **2021**, *103*, 054315. [CrossRef]
40. Zhang, K.; He, X.; Meng, J.; Pan, C.; Shen, C.; Wang, C.; Zhang, S. Predictive power for superheavy nuclear mass and possible stability beyond the neutron drip line in deformed relativistic Hartree-Bogoliubov theory in continuum. *Phys. Rev. C* **2021**, *104*, L021301. [CrossRef]
41. Pan, C.; Zhang, K.Y.; Chong, P.S.; Heo, C.; Ho, M.C.; Lee, J.; Li, Z.P.; Sun, W.; Tam, C.K.; Wong, S.H.; et al. Possible bound nuclei beyond the two-neutron drip line in the $50 \leq Z \leq 70$ region. *Phys. Rev. C* **2021**, *104*, 024331. [CrossRef]
42. Sun, X.X.; Zhou, S.G. Rotating deformed halo nuclei and shape decoupling effects. *Sci. Bull.* **2021**, *66*, 2072–2078. [CrossRef] [PubMed]
43. Choi, Y.B.; Lee, C.H.; Mun, M.H.; Kim, Y. Bubble nuclei with shape coexistence in even-even isotopes of Hf to Hg. *Phys. Rev. C* **2022**, *105*, 024306. [CrossRef]
44. Kim, S.; Mun, M.H.; Cheoun, M.K.; Ha, E. Shape coexistence and neutron skin thickness of Pb isotopes by the deformed relativistic Hartree-Bogoliubov theory in continuum. *Phys. Rev. C* **2022**, *105*, 034340. [CrossRef]

45. Zhang, K.; Yang, S.; An, J.; Zhang, S.; Papakonstantinou, P.; Mun, M.H.; Kim, Y.; Yan, H. Missed prediction of the neutron halo in 37Mg. *Phys. Lett. B* **2023**, *844*, 138112. [CrossRef]
46. Zhang, K.Y.; Papakonstantinou, P.; Mun, M.H.; Kim, Y.; Yan, H.; Sun, X.X. Collapse of the $N = 28$ shell closure in the newly discovered $^{39}$Na nucleus and the development of deformed halos towards the neutron dripline. *Phys. Rev. C* **2023**, *107*, L041303. [CrossRef]
47. Zhang, X.Y.; Niu, Z.M.; Sun, W.; Xia, X.W. Nuclear charge radii and shape evolution of Kr and Sr isotopes with the deformed relativistic Hartree-Bogoliubov theory in continuum. *Phys. Rev. C* **2023**, *108*, 024310. [CrossRef]
48. Guo, P.; Pan, C.; Zhao, Y.C.; Du, X.K.; Zhang, S.Q. Prolate-shape dominance in atomic nuclei within the deformed relativistic Hartree-Bogoliubov theory in continuum. *Phys. Rev. C* **2023**, *108*, 014319. [CrossRef]
49. Zhang, K.Y.; Zhang, S.Q.; Meng, J. Possible neutron halo in the triaxial nucleus $^{42}$Al. *Phys. Rev. C* **2023**, *108*, L041301. [CrossRef]
50. Mun, M.H.; Kim, S.; Cheoun, M.K.; So, W.; Choi, S.; Ha, E. Odd-even shape staggering and kink structure of charge radii of Hg isotopes by the deformed relativistic Hartree–Bogoliubov theory in continuum. *Phys. Lett. B* **2023**, *847*, 138298. [CrossRef]
51. Xiao, Y.; Xu, S.Z.; Zheng, R.Y.; Sun, X.X.; Geng, L.S.; Zhang, S.S. One-proton emission from 148–151Lu in the DRHBc+WKB approach. *Phys. Lett. B* **2023**, *845*, 138160. [CrossRef]
52. He, X.T.; Wu, J.W.; Zhang, K.Y.; Shen, C.W. Odd-even differences in the stability "peninsula" in the $106 \leq Z \leq 112$ region with the deformed relativistic Hartree-Bogoliubov theory in continuum. *Phys. Rev. C* **2024**, *110*, 014301. [CrossRef]
53. Lu, Q.; Zhang, K.Y.; Zhang, S.S. Triaxial shape of the one-proton emitter 149Lu. *Phys. Lett. B* **2024**, *856*, 138922. [CrossRef]
54. Pan, C.; Zhang, K.; Zhang, S. Nuclear magnetism in the deformed halo nucleus 31Ne. *Phys. Lett. B* **2024**, *855*, 138792. [CrossRef]
55. An, J.L.; Zhang, K.Y.; Lu, Q.; Zhong, S.Y.; Zhang, S.S. A unified description of the halo nucleus $^{37}$Mg from microscopic structure to reaction observables. *Phys. Lett. B* **2024**, *849*, 138422. [CrossRef]
56. Zhang, K.Y.; Pan, C.; Wang, S. Examination of the evidence for a proton halo in $^{22}$Al. *Phys. Rev. C* **2024**, *110*, 014320. [CrossRef]
57. DRHBc Mass Table Collaboration. Available online: http://drhbctable.jcnp.org/ (accessed on 1 October 2024).
58. Zhao, P.W.; Li, Z.P.; Yao, J.M.; Meng, J. New parametrization for the nuclear covariant energy density functional with a point-coupling interaction. *Phys. Rev. C* **2010**, *82*, 054319. [CrossRef]
59. Zhang, K.; Cheoun, M.K.; Choi, Y.B.; Chong, P.S.; Dong, J.; Geng, L.; Ha, E.; He, X.; Heo, C.; Ho, M.C.; et al. Deformed relativistic Hartree-Bogoliubov theory in continuum with a point-coupling functional: Examples of even-even Nd isotopes. *Phys. Rev. C* **2020**, *102*, 024314. [CrossRef]
60. Kucharek, H.; Ring, P. Relativistic field theory of superfluidity in nuclei. *Z. Phys. A* **1991**, *339*, 23–35. [CrossRef]
61. Zhou, S.G.; Meng, J.; Ring, P. Spherical relativistic Hartree theory in a Woods-Saxon basis. *Phys. Rev. C* **2003**, *68*, 034323. [CrossRef]
62. Ring, P.; Schuck, P. *The Nuclear Many-Body Problem*; Springer: New York, NY, USA, 1980.
63. Pan, C.; Zhang, K.; Zhang, S. Multipole expansion of densities in the deformed relativistic Hartree-Bogoliubov theory in continuum. *Int. J. Mod. Phys. E* **2019**, *28*, 1950082. [CrossRef]
64. Chatt, J. Recommendations for the naming of elements of atomic numbers greater than 100. *Pure Appl. Chem.* **1979**, *51*, 381–384.
65. Wang, S.; Guo, P.; Cong, P. Determining the ground state for superheavy nuclei from the deformed relativistic Hartree-Bogoliubov theory in continuum. *Particles* 11. *under review*.


**Disclaimer/Publisher's Note:** The statements, opinions and data contained in all publications are solely those of the individual author(s) and contributor(s) and not of MDPI and/or the editor(s). MDPI and/or the editor(s) disclaim responsibility for any injury to people or property resulting from any ideas, methods, instructions or products referred to in the content.